

ARTICLE

Miniature Boat Fabrication with Striking Loading Capacity in Seawater from Hydrophobic Steel Mesh

Zai-xing Jiang^{a†}, Ming-qiang Wang^{a†}, Hao Cheng^{a†}, Hai-bao Lv^b, Yong-tao Yao^b, Yong-ping Bai^a, Lu Shao^{a*}, Yu-dong Huang^{a*}

a. Department of Polymer Science and Technology, School of Chemical Engineering and Technology, Harbin Institute of Technology, Harbin 150001, China

b. Science and Technology on Advanced Composites in Special Environments Laboratory, Harbin Institute of Technology, Harbin 150080, China

(Dated: Received on March 16, 2015; Accepted on September 15, 2015)

A superhydrophobic steel mesh film was prepared by combination of macro-scale rough surface and low surface energy material treatment through a facile coating method. The contact angle for seawater is measured to be as high as 130.16°. A reformed Cassie-Baxter equation was applied for the theoretical predictions of this novel material for the first time. Good agreement between the predictions and experiments was obtained. The loading capacities of these boats, fabricated from the resulting hydrophobic steel meshes, were also characterized. The highest loading weight about 17.50 g was obtained by the steel mesh treated by 2.0wt% (heptadecafluoro-1,1,2,2,-tetradecyl)trimethoxysilane solution. The striking loading capacity of this miniature boat may be attributed to the air film trapped around the mesh surface. This novel superhydrophobic steel mesh material have wide applications on medical materials, marine materials and smart materials.

Key words: Hydrophobic, Steel mesh, Loading capacity

I. INTRODUCTION

In recent years, inspired by water-repellent lotus leaves with hierarchically rough structures coated with a waxy layer [1, 2], researchers pay more and more attentions to superhydrophobic surfaces, because of their wide applications, such as self-cleaning material and antifogging material. Superhydrophobic surfaces can also been used to improve the corrosion resistance of metal in seawater. These surfaces have high water contact angle, low contact angle hysteresis [2, 3] and these surfaces are produced by combinations of lowering the surface free energy and enhancing the surface roughness. Moreover, a superhydrophobic mesh has unique characteristics, such as big porous surface, mesh-like geometry, high pressure resistance, and high striking loading capacity. However, few attentions are paid to the loading capacity of hydrophobic mesh in seawater.

Here, we fabricated a hydrophobic steel mesh surface based on the mimicking of macroscopic surface structure of asparagus setaceus branches, and studied its loading capacity in seawater. The hydrophobic steel meshes were prepared by grafting low

surface tension materials of (heptadecafluoro-1,1,2,2,-tetradecyl)trimethoxysilane (HFTES). The wetting behaviors of the hydrophobic steel meshes in seawater were characterized by contact angle measurement. A reformed Cassie-Baxter model was derived and used to predict the superhydrophobicities of the steel meshes. Furthermore, the characterization of these hydrophobic steel meshes was also performed. The steel meshes used here was the common steel wire mesh which is cheap and easy to get. The treated method is also facile, cheap and easy performed. Thus, the fabricated steel meshes have great potential application in industrial productions, and have broad applications in many areas, such as aquatic robots, environmental surveillance, marine corrosion, heart supporter, and microfluidity.

II. EXPERIMENTS

A. Materials

The steel meshes used in this study were obtained from Hebei Anhua Hardware & Mesh Product Co., Ltd. The pore size of the mesh used was about 220 $\mu\text{m} \times 220 \mu\text{m}$.

(Heptadecafluoro-1,1,2,2,-tetradecyl)trimethoxysilane (HFTES), provided by Dow Corning Co., Ltd., was dissolved in a mixture of ethanol and ultrapure water. HFTES was 0.5wt%, 1.0wt%, 2.0wt%, 4.0wt%, and

[†]These authors contributed equally to this work.

*Authors to whom correspondence should be addressed. E-mail: huangyd@hit.edu.cn, jzx1981@163.com, Tel./FAX: +86-451-86414806

8.0wt%. Then the solutions were treated in an ultrasonic bath at room temperature for 30 min. Finally, these solutions were used to treat steel meshes.

B. Fabrication of hydrophobic steel mesh and miniature mesh boat

The steel mesh was successively washed in an ultrasonic bath with acetone for 5 min, ultra-pure water for 5 min, and 1.0 mol/L NaOH for 5 min to remove surface impurities. After being cleaned by ultra-pure water in ultrasonic bath for 10 min and dried for 30 min in ambient temperature, these mesh films were immersed into HFTEs solution. After that, the mesh films were heat treated at 100 °C in air for 3 h. The treated steel mesh films were cut to a size of 60 mm×55 mm. The above obtained steel mesh film was folded into a boat of 40 mm×35 mm×10 mm.

C. Contact angle measurements

Contact angles were measured to study the hydrophobic properties of the treated steel mesh surfaces. The contact angles on the prepared steel mesh surfaces with sessile water drops were monitored using a Sony digital camera (DSC-W290, Sony Corporation, Japan), and were calculated using a contact angle meter (the First Optics Factory, Chuangchun, China). The volume of the applied drops of ultrapure water was 10 μL. Droplets were placed at five positions for one sample and the averaged value was adopted as the contact angle.

D. Loading capacity evaluation

The maximum loading capacity of each miniature boat was measured according to Ref.[20]. Silver sand and water were carefully added into the columnar container until the upper edges of the mesh boat were flooded by water and the boat started to sink. The columnar container was placed at the center of the mesh boat. Then the silver sand and the container were weighed. The sum weight of silver sand and container are the maximum loading weight of the mesh boat.

III. RESULTS AND DISCUSSION

It is well known that the characterization of hydrophobic is examined through the measurement of contact angle. According to the Michielsens' analysis, the roughness of the surface in contact with seawater is the length of the chord in contact with water, $R\beta$ divided by the projected area of the chord in contact with seawater, $R\sin\beta$, *i.e.* $R_f = \beta/\sin\beta$, where R is radius of the seawater in contact with the steel mesh β is the angle between

the top of the cylinder and the liquid contact line [23, 24]. Then, following Marmur's derivation, the length f of the red area in Fig.1(a) divided by the project area is calculated as:

$$f = \frac{2R \sin \beta L}{4(R+d)(R+L)} \quad (1)$$

Substituting f and R_f for case into Eq.(1) results in [26]:

$$\cos \theta^{CB} = -\frac{R\beta \cos \beta}{R+d} + \frac{R \sin \beta}{R+d} - 1 \quad (2)$$

Following Marmur's derivation, $d(R_f f)/df = (\cos \beta)^1$ and $d^2(R_f f)/df^2 > 0$. Under these conditions, Marmur showed that there was a minimum in the surface free energy on each surface such that $\beta = \pi - \theta_e$. Substituting it for β , the following equation is obtained:

$$\cos \theta^{CB} = \frac{R(\pi - \theta_e) \cos \theta_e}{R+d} + \frac{R \sin \theta_e}{R+d} - 1 \quad (3)$$

Following Eq.(3), the reformed original Cassie-Baxter model, the contact angles of steel meshes with different pore sizes are calculated after determination of the parameters of θ_e , R and d . The contact angle of clean and smooth steel film surface is measured to be 53.2°. In order to make the film surface hydrophobic, the HFTEs with different concentrations were grafted onto the steel film surfaces. As the value of θ_e is determined.

The mesh exhibit the square shape and length of mesh is about 220 μm. The radius of the steel wires is about 120 μm. Substituting these values into Eq.(3) along with the measured contact angles from the flat steel films, we find the predicted contact values, as shown in Fig.1(b). Based on Eq.(3), in order to fabricate the superhydrophobic steel mesh, the θ_e should be larger than 117.9°. While there is no θ_e larger than 117.9°, so it is predicted that no superhydrophobic mesh will be obtained. The measured contact angles of the seawater are also shown in Fig.1(b). And the tilt-view photographs for seawater droplet sat on treated steel mesh surface are shown in Fig.1 (c)–(g). In addition, The measured contact angles and the tilt-view photographs for water droplet are also provided in Fig.S1 and Fig.S2(a)–(e) (in supplementary materials).

Though the superhydrophobicity of steel meshes are not achieved, the hydrophobic steel meshes are widely obtained. As seen in Fig.1(b), these values are in good agreement with the measured values, though the measured values are slightly higher than our predicted values, due to the real average value of d being lower than the values chosen in this analysis. For example, the length of square of the mesh is higher than that we chose. This is due to the non-homogenous of pore size. As shown earlier, lower values of d will result in lower values of θ^{CB} . Thus the measured values of θ^{CB} are greater than the predicted values. Furthermore, it is should be noted that the measured values are also lower

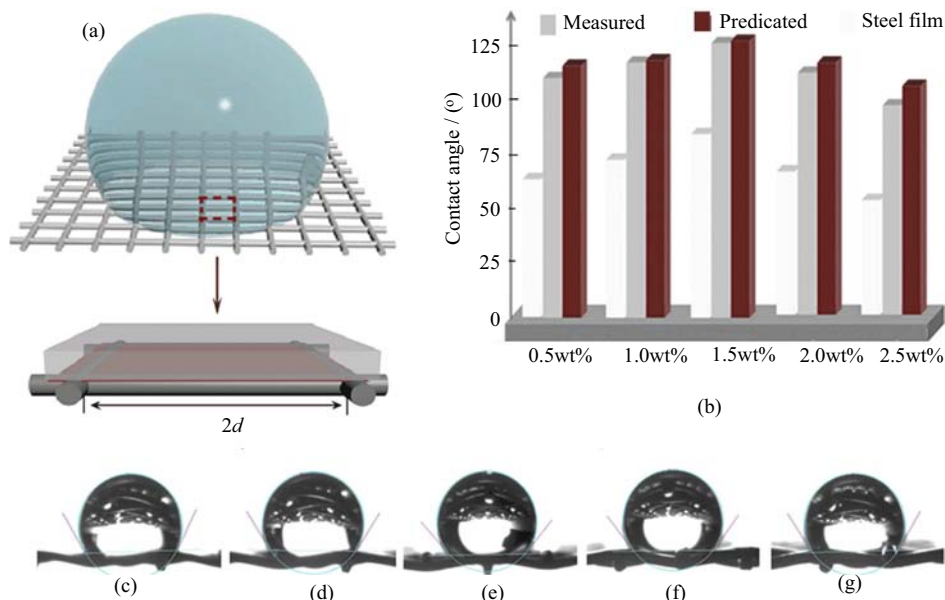


FIG. 1 (a) Schematic plan of water drop sitting on steel mesh. The red area represents the projected area of the steel wires in contact with water. (b) Comparison of measured values and predicted values. (c)–(g) Tilt-view photographs for seawater droplet sat on treated steel mesh surface. (c) 0.5wt% HFTES treated. (d) 1.0wt% HFTES treated. (e) 2.0wt% HFTES treated. (f) 4.0wt% HFTES treated. (g) 8.0wt% HFTES treated.

than the real contact angles, due to the existence of H , as shown in Fig.1(a). Though the water or seawater cannot wet the steel wire, water or seawater drops will somewhat have contact with steel wire because of the gravity. Thus, in the measurement of contact angles through its two dimension photos, the bottom margin (the red area as shown in Fig.1(a)) cannot be seen, which leads to the low measured contact angles.

As discussed above, the fabricated steel meshes have the hydrophobicity, *i.e.* the interface of steel filament and water cannot take place of the interface of steel filament and air, and accordingly, the water or seawater can rest on the surface of steel mesh with the aid of surface tension. According to the reformed Cassie-Baxter model, there will be air film formation when the water or seawater cannot wet the rough surface. Thus, there are air films around the steel meshes when they contact with water or seawater.

The formation of air films can generate many amazing phenomenon. A wonder phenomenon is that the miniature boat fabricated with hydrophobic steel meshes not only can float on seawater surface but also has remarkable loading capacity. Optical images of a miniature boat floating on seawater surface (treated with 8.0wt% HFTES solution) are shown in Fig.2. As shown in Fig.2, the miniature boat can freely float on seawater surface, and the seawater does not penetrate into the boat during the process of loading weight. Furthermore, it can be seen that the boat can keep floating even though its upper edges are below the horizontal surface. In addition, in the process of this work, it is found that the boat will have obvious movement with weak force.

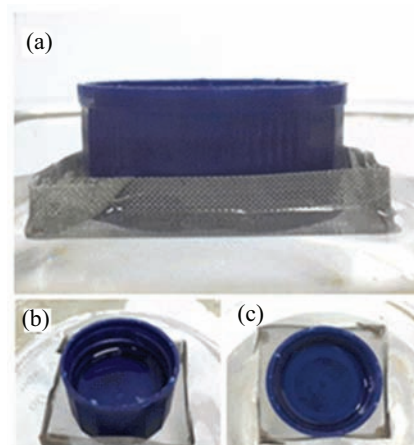


FIG. 2 Optical images of a miniature boat floating on seawater surface (treated with 8.0 wt% HFTES solution). (a) Top view, (b) and (c) side views.

The maximal loading capacities of the resulting boats are calculated through quantifying the loaded water, as shown in Fig.3. Here, it should be noted that the untreated steel mesh boat cannot float over the seawater surface, so it has no loading capacity and the following discussions about loading capacity all refer to the treated steel mesh boat. The miniature boat fabricated from steel mesh treated with 2.0wt% HFTES solution has the largest loading capacity, while miniature boat treated with 0.5wt% HFTES solution has the lowest loading capacity. It is observed that the loading capacities change become moderate when the concentration

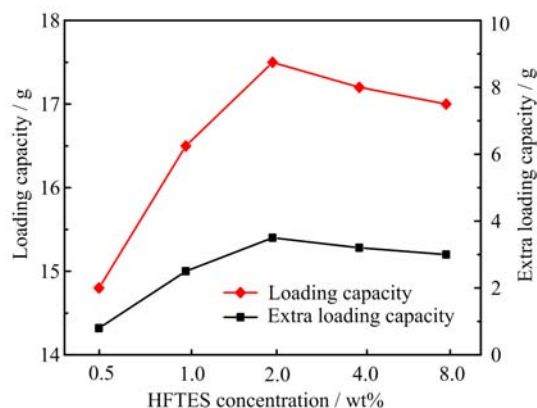


FIG. 3 Effect of HFTES concentration on the mesh loading capacities.

of HFTES is higher than 2.0wt%. This may be because that surface topography will be changed with the HFTES concentration increase, *i.e.* the two wires are bonded together. And the abundant HFTES may also provide extra buoyancies. Interestingly, take steel mesh boat (treated with 2.0wt% HFTES solution) as an example, the maximal loading weight is about 16 times greater than the weight of the boat itself, which can be hardly achieved when the similar boat is made by steel sheet.

As is demonstrated above, the steel mesh boats, which can float over seawater surface, has striking loading capacities. The large loading capacities of these boats arise from their hydrophobic surfaces. Owing to the hydrophobic steel mesh surface, an air layer will surround the steel mesh surfaces, which prevents the boats from being wetted and/or penetrated by seawater. Furthermore, the loading capacities of these treated boats are all larger than 14.10 g, which exceed the maximum buoyancy force calculated for the boat (*i.e.* 14.10 g). The maximal extra loading weights of resulting steel mesh boats are shown in Fig.3. The highest extra loading weight (3.50 g) can be achieved with the steel mesh boat treated with 2.0wt% HFTES solution. The extra loading capacities are also attributed to the existence of air film.

In addition, we found that the steel mesh boats also have a striking loading capacity in water (Fig.S3 in supplementary materia). When the steel mesh boats were treated with 2.0wt% HFTES, the loading weight could reach 18.4 g (Fig.S3(c) in supplementary material) which was larger than that in seawater. According to the Eq.(5), the maximum buoyancy force calculated for the boat in the water is 14.00 g. Hence, the highest extra loading weight (4.40 g) can be achieved with the steel mesh boat treated with 2.0wt% HFTES solution. Due to the extra loading weight as the most index to measure the loading capacity of the steel mesh boats, the loading capacity of the steel mesh boats in the water is superior to that of in the seawater. This phenomenon

can be attributed to that the salt has an influence on the interfacial tension of the water. It turns out that the steel not can carry more weight than in the water.

On the basis of the above analysis, the loading weight of the steel mesh boat can be divided into three parts [23]: the first contribution to the loading capacity is the buoyancy force (F_{III}) related to boat volumes; the second contribution is sufficient additional buoyancy force produced by the air surround the boat (F_{II}), which is the source of extra loading capacity of the steel mesh boat; the third part is the weight of the boat itself (F_{IV}). Thus, the loading weight (F_I) of the boat having a size of $l \times w \times h$ (l is length, w is width, and h is height) can be expressed as follows:

$$F_I = F_{III} + F_{II} - F_{IV} = \rho g l w h + \rho g [l w + 2(l h + w h)] H - m g \quad (4)$$

here, g is the gravitational constant, and H is the thickness of the air film. And the extra supporting force (F_{II}) for a boat can be illustrated as:

$$F_{II} = \rho g [l w + 2(l h + w h)] H \quad (5)$$

Thus, from Eq.(5), H can be calculated. H is 0.31–1.52 mm for the treated steel mesh boats, *i.e.* there is air film with thickness of 0.31–1.52 mm around the treated steel mesh boats. If there is no air film, water will permeate into the boat.

In summary, a novel mesh film with hydrophobic property was prepared by the combination of macro-scale rough surfaces and low surface energy material treatment. The predicted values based on the reformed Cassie-Baxter equation are in good agreement with the measured values. Furthermore, the loading capacities of these hydrophobic meshes are also performed. The steel mesh boats not only can float freely on seawater surface but also exhibit large loading capacities, and the highest loading weight, 17.50 g, is achieved when the treated concentration of HFTES solution is 2.0wt%. The striking loading capacities of these miniature boats are attributed to the air film trapped around the mesh surface. The present finding is suitable for many practical applications, and can be expanded to design novel superfloating and dragreducing aquatic devices.

Supplementary materials: The wetting behaviors of the hydrophobic steel meshes in water were also investigated. Figure S1 shows the comparison of measured values and predicted values of the steel meshes in water. The Tilt-view photographs for water droplet sat on treated steel mesh surface were also investigated, as shown in Fig.S2. Moreover, Fig.S3 compares the loading capacities of the miniature boat which was fabricated by superhydrophobic steel mesh film treated with different HFTES solution. The results showed that the miniature boat exhibited good hydrophobic performance not only in seawater, but also in water.

IV. ACKNOWLEDGMENTS

This work was supported by the National Natural Science Foundation of China (No.51003021), the China Postdoctoral Science Special Foundation (No.201003420 and No.20090460067), UTC Exploration Project (No.CASC-HIT12-1C03), and the Harbin City Science and Technology Projects (No.2013DB4BP031). The authors would also like to thank Guo-jian Cao from Harbin University of Science and Technology for the TEM work.

- [1] W. Barthlott and C. Neinhuis, *Planta* **202**, 1 (1997).
- [2] H. Y. Erbil, A. L. Demirel, Y. Avci, and O. Mert, *Science* **299**, 1377 (2003).
- [3] R. Furstner and B. Wilhelm, *Langmuir* **21**, 956 (2005).
- [4] C. Yannick, J. Sebastien, A. Ahmed, B. Ralf, G. Leon, P. Edmond, and B. Rabah, *Langmuir* **23**, 1608 (2007).
- [5] A. B. D. Cassie and S. Baxter, *Trans. Faraday Soc.* **40**, 546 (1944).
- [6] P. Roura and J. Fort, *Langmuir* **18**, 566 (2002).
- [7] X. Zhang, F. Shi, J. Niu, Y. G. Jiang, and Z. Q. Wang, *J. Mater. Chem.* **6**, 621 (2008).
- [8] H. M. Shang, Y. Wang, K. Takahashi, and G. Z. Cao, *J. Mater. Sci.* **40**, 3587 (2005).
- [9] A. Satyaprasad, V. Jain, and S. K. Nema, *Appl. Surf. Sci.* **253**, 5462 (2007).
- [10] Z. G. Guo, W. M. Liu, and B. L. Su, *J. Colloid Interf. Sci.* **353**, 335 (2011).
- [11] S. A. Kulinich and M. Farzaneh, *Appl. Surf. Sci.* **230**, 232 (2004).
- [12] N. J. Shirtcliffe, G. Mchale, M. I. Newton, and C. C. Perry, *Langmuir* **21**, 937 (2005).
- [13] M. W. Cao, X. Y. Song, J. Zhai, J. B. Wang, and Y. L. Wang, *J. Phys. Chem. B* **110**, 13072 (2006).
- [14] T. L. Sun, G. J. Wang, H. Liu, L. Feng, L. Jiang, and D. B. Zhu, *J. Am. Chem. Soc.* **125**, 14996 (2003).
- [15] D. H. Xu, H. Liu, L. Yang, and Z. G. Wang, *Carbon* **44**, 3226 (2006).
- [16] S. L. Li, H. J. Li, X. B. Wang, Y. L. Song, Y. Q. Liu, L. Jiang, and D. B. Zhu, *J. Phys. Chem. B* **106**, 9274 (2002).
- [17] K. S. L. Kenneth, B. Jose, B. K. T. Kenneth, C. Manish, A. J. A. Gehan, I. M. William, H. M. Gareth, and K. G. Karen, *Nano Lett.* **3**, 1701 (2003).
- [18] E. Hosono, S. Fujihara, I. Honma, and H. S. Zhou, *J. Am. Chem. Soc.* **127**, 13458 (2005).
- [19] M. H. Yu, G. T. Gu, W. D. Meng, and F. L. Qing, *Appl. Surf. Sci.* **253**, 3669 (2007).
- [20] Q. M. Pan and M. Wang, *Appl. Mater. Interf.* **1**, 420 (2009).
- [21] M. Nosonovsky and B. Bhushan, *Microsyst. Technol.* **12**, 273 (2006).
- [22] M. Nosonovsky and B. Bhushan, *Microsyst. Technol.* **11**, 535 (2005).
- [23] S. Michielsen and H. J. Lee, *Langmuir* **23**, 6004 (2007).
- [24] A. Marmur, *Langmuir* **19**, 8343 (2003).